LIGHT POLLUTION

Citizen scientists report global rapid reductions in the visibility of stars from 2011 to 2022

Christopher C. M. Kyba,[1,2]* Yiğit Öner Altıntaş,[1]† Constance E. Walker,[3] Mark Newhouse[4]

The artificial glow of the night sky is a form of light pollution; its global change over time is not well known. Developments in lighting technology complicate any measurement because of changes in lighting practice and emission spectra. We investigated the change in global sky brightness from 2011 to 2022 using 51,351 citizen scientist observations of naked-eye stellar visibility. The number of visible stars decreased by an amount that can be explained by an increase in sky brightness of 7 to 10% per year in the human visible band. This increase is faster than emissions changes indicated by satellite observations. We ascribe this difference to spectral changes in light emission and to the average angle of light emissions.

Over much of Earth's land surface, the night sky no longer fully transitions to starlight and moonlight after sunset (*1*). Instead, the sky also glows with an artificial twilight caused by the scatter of anthropogenic light in the atmosphere (*2*). The radiance of skyglow grew exponentially for much of the 20th century (*3*) as a result of population growth, expansion of settlements, and deployment of new lighting technologies (*4*, *5*). The character of the night sky is now different from what it was when life evolved and civilization developed.

Many of the behavioral and physiological processes of life on Earth are connected to daily and seasonal cycles. For example, visual predation requires sufficient light to see, and predator–prey interactions are therefore expected to be affected by skyglow (*6*). There are few controlled field studies of the ecological impacts of skyglow, but it has been have shown to affect plants, animals, and their interactions (*7*), and laboratory studies have demonstrated changes in the physiology of fish at skyglow-like nighttime illuminance of 0.01 lux (*8*). In addition to its environmental consequences, skyglow limits human observation of starry skies and the Milky Way. The increase in skyglow has affected human culture (*9*), not only by restricting stargazing and astronomy but also by changing the overall appearance of the night sky.

Effective methods for reducing light pollution are well understood (*10*, *11*), and many of them also reduce electricity consumption. These measures have been implemented on local scales (*12*, *13*) but have not seen widespread adoption. Nevertheless, awareness of light pollution has led some policy-makers to introduce measures that attempt to control light pollution (*14*).

During the 2010s, many outdoor lights were replaced by light-emitting diodes (LEDs): Global LED market share for new general lighting grew from under 1% in 2011 to 47% in 2019, and LED market share for new outdoor lighting in the United States was 66% in 2020 (*15*). The impact on skyglow from this transition to LEDs is unclear. Some researchers have predicted that it will be beneficial (*16*); others, that it could be harmful because of spectral changes (*17*) or a rebound effect (*18*), in which the high luminous efficacy (more light emitted for a given power) of LEDs leads to more or brighter lights being installed or longer hours of operation.

The generation of skyglow and changes in its character are related to social, economic, and technological processes, and we therefore expect skyglow trends to differ within and across countries. Time-series measurements of skyglow from individual sites, although useful for some purposes, might not be representative of how skyglow is changing on larger scales. It would therefore be beneficial to measure changes in skyglow on continental and global scales.

In principle, it is possible to directly measure skyglow through satellite observations of Earth at night (*19*). Unfortunately, the only satellite instruments that currently monitor the whole Earth have limited resolution and sensitivity and cannot detect light with wavelengths below 500 nm (*20*). This is a problem for three reasons: (i) Shorter wavelengths scatter more effectively in the atmosphere, increasing the chance that a photon emitted upward returns to Earth as skyglow (*2*); (ii) LEDs marketed as white usually have an emission peak between 400 and 500 nm, where the satellite sensor is insensitive; and (iii) human visual sensitivity shifts toward shorter wavelengths at night (*11*). The first two effects could mean that changes in ground radiance observed by satellite (*21*, *22*) differ from changes in skyglow. The third effect means that ground-based radiometers (and photometers) face a similar problem: If skyglow darkens at longer wavelengths but brightens at shorter wavelengths, it would be unclear whether the number of stars visible to humans would increase or decrease (*23*, *24*).

We analyzed a citizen science dataset in which the human visual system was directly used as a sensor (*24*, *25*). In the Globe at Night

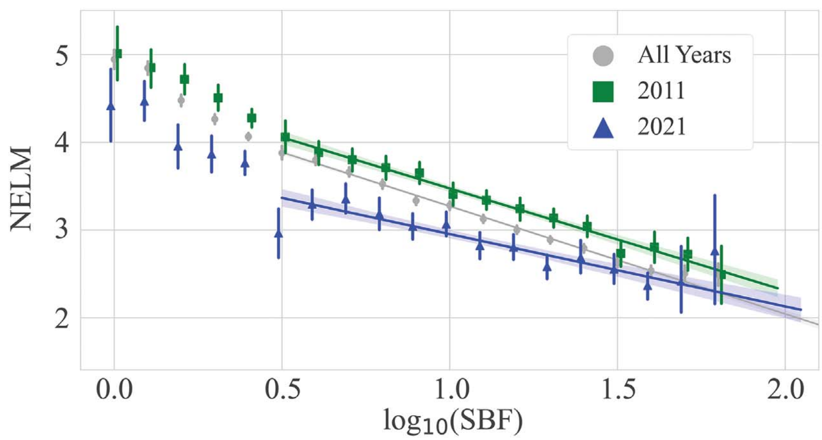

Fig. 1. Naked eye limiting magnitude estimated by Globe at Night participants as a function of the night sky brightness in 2014. The sky brightness factor (SBF) is the ratio of total radiance to natural sky radiance, so SBF = 1 indicates starlight and SBF = 10 (plotted as $\log_{10}$SBF = 1) indicates that the sky is 10 times as bright as starlight (plotted as $\log_{10}$SBF = 0 and 1, respectively (*26*). The relationship is shown for 2011 (green squares), 2021 (blue triangles), and the average of all years from 2011 to 2022 (gray circles). Smaller NELM values mean that fewer stars are visible. Lines indicate linear models fitted to the data for $\log_{10}$SBF >0.5, which corresponds to ~3 times as bright as starlight. Shaded regions show the 95% confidence interval.

[1]Remote Sensing and Geoinformatics, Deutsches GeoForschungsZentrum Potsdam, 14473 Potsdam, Germany. [2]Geographisches Institut, Ruhr-Universität Bochum, 44780 Bochum, Germany. [3]Office of Observatory Site Protection, National Optical-Infrared Astronomy Research Laboratory, Tucson, AZ 85719, USA. [4]Communications, Education and Engagement, National Optical-Infrared Astronomy Research Laboratory, Tucson, AZ 85719, USA.
***Corresponding author. Email: kyba@gfz-potsdam.de**
†Present address: European Organization for the Exploitation of Meteorological Satellites, 64295 Darmstadt, Germany.

Table 1. Summary of results for different geographic areas. Best-fitting values of our model are listed for three continental groupings and the global average. $\hat{r}$ is the rate of increase, $\hat{N}_n$ is the NELM for natural skies, $\hat{s}$ relates NELM to the World Atlas, σ is the standard deviation of residuals, and E is the error rate (*26*). Uncertainties are ±1 standard deviation and are statistical only. Rest of World includes four continents because of insufficient coverage (see text). More detailed results, before combining continents, are listed in table S1.

Region	$\hat{r}$ (%)	$\hat{N}_n$ (NELM)	$\hat{s}$	σ (NELM)	E (%)
Europe	6.5 ± 1.0	4.77 ± 0.03	−1.33 ± 0.03	0.953 ± 0.012	2.4 ± 0.5
North America	10.4 ± 0.5	4.95 ± 0.02	−1.52 ± 0.02	1.009 ± 0.008	1.7 ± 0.3
Rest of World	7.7 ± 0.7	4.66 ± 0.03	−1.37 ± 0.02	1.077 ± 0.011	2.5 ± 0.5
Global average	9.6 ± 0.4	4.825 ± 0.014	−1.429 ± 0.014	1.022 ± 0.006	2.1 ± 0.2

project [operated by the National Optical-Infrared Astronomy Research Laboratory (NOIRLab)], participants are presented with a set of star maps (example shown in fig. S1) and asked which one best matches the night sky at their location (*26*). This provides an estimate of the naked eye limiting magnitude (NELM), the visual apparent magnitude of the faintest star that can be seen. Astronomical magnitudes are an inverted logarithmic scale, so the NELM is smaller for brighter skies. The NELM is related to skyglow because as background radiance increases, faint point sources of light become invisible (*27*). The limiting magnitude estimated by citizen scientists using this method correlates with the locations of skyglow determined using satellite datasets (*24*, *25*). We grouped different regions of the globe according to their sky brightness in 2014, as determined by the (satellite-based) World Atlas (*1*), to examine how the NELMs in similarly bright areas change over time (Fig. 1 and fig. S2).

Our method (*26*) accounts for differences in the set of citizen scientists participating each year (Fig. 2) and allows us to measure changes in stellar visibility on global or continental spatial scales. The overall number of observations limits the spatial and temporal scales over which trends can be determined (particularly for developing countries, where rapid skyglow change is suspected but little observational evidence is available). The Globe at Night data have a spatial bias toward Europe, North America (especially the United States), and a small number of other countries; there is also a bias toward inhabited areas. For example, 50.6% of the Asian contributions are from Japan, and contributions from Australia are overwhelmingly from coastal areas (Fig. 2B and fig. S3) during 2020 (Fig. 2A). Because Europe and North America have sufficient data in both time and space, we report trends for those continents and combine all the others (referred to as Rest of World hereafter).

Although this dataset does not represent an average of either the land area or human population distribution, participants are concentrated in regions where skyglow is most prevalent (*1*). The global trend in skyglow that we measure likely underestimates the trend in countries with the most rapid increases in economic development, because the rate of change in light emission is highest there (*21*) and we expect the addition of new lights to have a greater impact on skyglow than would result from the replacement of existing lights.

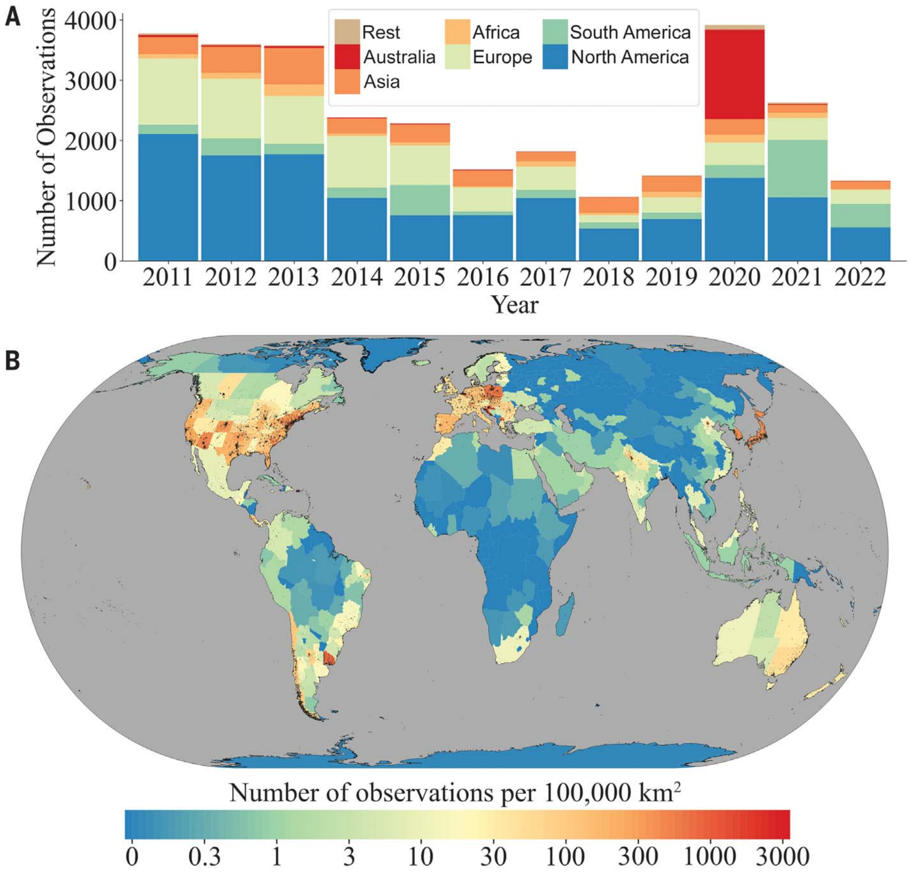

Fig. 2. Participation in Globe at Night from January 2011 to August 2022. (**A**) Bar chart showing the temporal distribution. Participation for each year is subdivided by continent, as indicated in the legend. (**B**) Spatial distribution of all years combined, on an equal-area Eckert IV map projection. Colors indicate the participation normalized by land area, on a logarithmic scale. Black points show the locations of individual observations (more visible in fig. S3). Some of the largest countries have been divided into smaller jurisdictions.

To convert the NELM measurements to rates of change in effective skyglow radiance for human vision, we fitted a model to a subset of the dataset [observations from January 2011

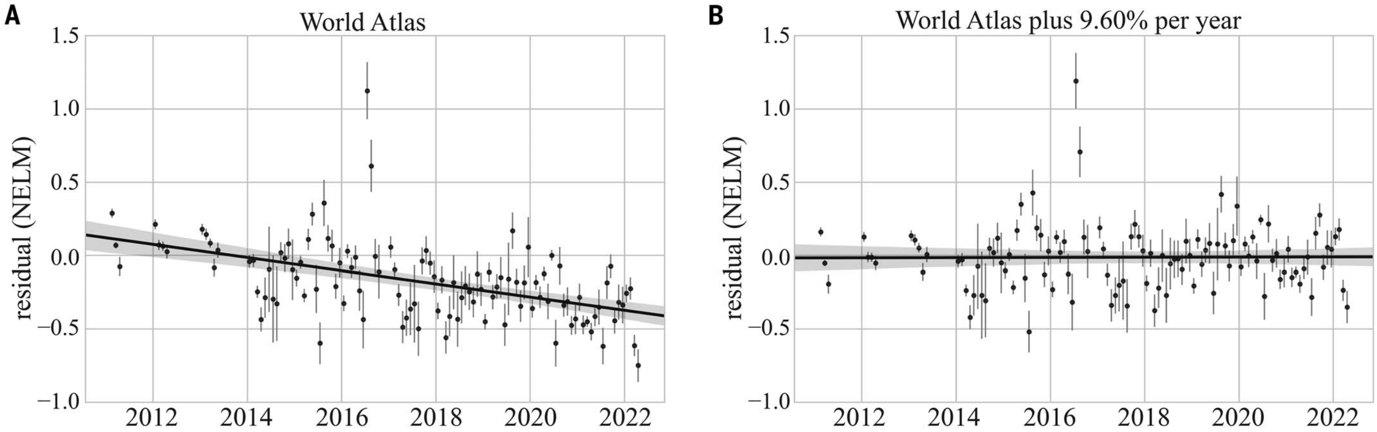

Fig. 3. Difference from expected limiting magnitude under different skyglow growth models. The monthly residuals (observed minus expected) between reported NELM and the expectation based on the World Atlas (Fig. 1) under two models: (**A**) the standard 2014 World Atlas; (**B**) the World Atlas radiance multiplied by an exponential increase of 9.6% per year relative to January 2014 (*26*). Positive residuals indicate that observers reported more stars than expected. Error bars show the standard error, and data points before 2014 include higher numbers of observations than those made after 2014. Black lines show a linear model fitted to the residuals, and the shaded region shows the 95% confidence interval.

to August 2022, without twilight, moonlight, or reported snow on the ground (*26*)], using a maximum likelihood method. There are five free parameters in the model: (i) the average limiting magnitude reported in regions with no light pollution (y intercept in Fig. 1); (ii) the slope of the relationship between NELM and World Atlas skyglow radiance (similar to the slope in Fig. 1, but with a time-adjusted radiance); (iii) the annual rate of change in artificial skyglow; (iv) the standard deviation in the residuals between measured and predicted NELM; and (v) an estimate of the error rate in the Globe at Night dataset (e.g., due to participants reporting their location or NELM incorrectly).

We find that the change in the number of visible stars reported by Globe at Night participants is equivalent to a 9.6% per year annual increase in sky brightness, averaged over the locations of participants (Table 1). For an 18-year period (such as the duration of a human childhood), this rate of change would increase sky brightness by more than a factor of 4. A location with 250 visible stars would see that number reduce to 100 visible stars over the same period. Because our method uses measurements made with human vision, it accounts for changes in both the radiance and spectrum of the night sky.

We confirmed this finding by performing an alternative analysis of the data. Instead of using a maximum likelihood method to fit a model of the skyglow change, we performed least-squares fitting of a linear model to the monthly (observed minus expected) NELM residuals under the assumption that skyglow remains constant (Fig. 3A) or increases at a rate of 9.6% per year (Fig. 3B). The best-fitting rate of change in NELM residuals is −0.044 ± 0.007 magnitude per year for the uncorrected model and 0.001 ± 0.007 magnitude per year for the model corrected for skyglow increase. The even distribution of points above and below zero in the corrected model shows that the trend is not being driven by outliers at the start or end of the analysis period (Fig. 3B).

The rate of skyglow increase that we find is much larger than the rates of growth in light emissions observed by satellite in the 500- to 900-nm band, which were 2.2% per year globally during 2012–2016 (*21*) and >1.6% per year during 1992–2017 (with the possibility of faster increases in the visual band from 2012 onward) (*22*). For a more direct comparison, we analyzed the satellite radiance trends at the Globe at Night observation locations during 2014–2021 (*26*). Even after controlling for the locations, rates of change in upward radiance measured by satellite were also much smaller than our calculated rate of skyglow increase (table S2). For example, for North America during 2011–2021, we find the rate of increase in skyglow radiance is 10.4 ± 0.5%, compared to −0.80 ± 0.04% in the surface radiance measured by satellite at these locations during 2014–2021 (table S2). We ascribe the smaller satellite radiance change at Globe at Night locations compared to that found in other studies (*21*, *22*) to the tendency of Globe at Night participants to observe from residential areas (see materials and methods).

These different results are not incompatible, because there are several differences between observing surface radiance with satellites and sky radiance as seen by humans on the ground. For example, the widespread conversion of streetlights from gas discharge lamps to LEDs (*16*, *28*) could result in spectral changes that affect the two datasets differently, as discussed above. If luminance is maintained after converting street lighting to LEDs, the spectral shift toward shorter-wavelength (bluer) light causes the radiance observed by the satellite to decrease (*17*). By contrast, skyglow mesopic luminance after installation of LEDs could potentially either increase as a result of increased atmospheric scattering of blue light (*2*, *29*) or decrease as a result of improved lighting fixtures that reduce horizontal emission (*16*).

The contributions to ground-observed skyglow and satellite-observed surface radiance depend on the lighting type. Most satellite radiometers have little to no sensitivity to light emitted toward the horizon (e.g., from a window or self-luminous sign) (*30*). However, light propagating toward the horizon is the largest contributor to skyglow because of its longer path length (by an order of magnitude) from ground to space at such angles. In the early evening, a large fraction of the light that escapes cities is emitted by sources other than streetlights (*31*). Some of these lighting applications, such as decorative and advertising lighting, produce a larger fraction of horizontally propagating light than modern street lighting does. It is therefore likely that some of the differences between the rates of change for skyglow that we calculate and those estimated from satellite data arise from changes in lighting practices or deployment.

We draw two conclusions from these results. First, the visibility of stars is deteriorating rapidly, despite (or perhaps because of) the introduction of LEDs in outdoor lighting applications. Existing lighting policies are not preventing increases in skyglow, at least on continental and global scales. Second, the use of naked-eye observations by citizen scientists provides complementary information to the satellite datasets.

REFERENCES AND NOTES

1. F. Falchi *et al*., *Sci. Adv.* **2**, e1600377 (2016).
2. J. C. Barentine, *Nat. Astron.* **6**, 1120–1132 (2022).
3. F. Hölker *et al*., *Ecol. Soc.* **15**, 13 (2010).
4. K. W. Riegel, *Science* **179**, 1285–1291 (1973).
5. J. Y. Tsao, P. Waide, *Leukos* **6**, 259–281 (2010).
6. C. C. M. Kyba, F. Hölker, *Landsc. Ecol.* **28**, 1637–1640 (2013).
7. A. A. Wilson *et al*., *Integr. Comp. Biol.* **61**, 1122–1133 (2021).
8. F. Kupprat, F. Hölker, W. Kloas, *Environ. Pollut.* **262**, 114324 (2020).
9. T. Gallaway, *J. Econ. Issues* **44**, 71–88 (2010).
10. O. P. Cleaver, Control of coastal lighting in anti-submarine warfare. *Tech. Rep.*, Engineer Board, Fort Belvoir, VA (1943). Report No. 746, GN 373 (accessed 16 May 2019).
11. F. Falchi, P. Cinzano, C. D. Elvidge, D. M. Keith, A. Haim, *J. Environ. Manage.* **92**, 2714–2722 (2011).
12. M. Aubé, J. Roby, *J. Quant. Spectrosc. Radiat. Transf.* **139**, 52–63 (2014).
13. R. F. Green, C. B. Luginbuhl, R. J. Wainscoat, D. Duriscoe, *Astron. Astrophys. Rev.* **30**, 1 (2022).
14. M. Morgan-Taylor, in *Urban Lighting, Light Pollution and Society*, J. Meier *et al*., Eds. (Routledge, 2015), chap. 9, pp. 159–176.
15. G. Zissis, P. Bertoldi, T. Serrenho, Update on the status of LED-lighting world market since 2018. *Tech. Rep.* (2021). https://data.europa.eu/doi/10.2760/759859.
16. B. Kinzey *et al*., An investigation of LED street lighting's impact on sky glow. *Tech. Rep.*, US Department of Energy (2017). PNNL-26411.
17. L.-W. Hung, S. J. Anderson, A. Pipkin, K. Fristrup, *J. Environ. Manage.* **292**, 112776 (2021).
18. J. Y. Tsao, H. D. Saunders, J. R. Creighton, M. E. Coltrin, J. A. Simmons, *J. Phys. D Appl. Phys.* **43**, 354001 (2010).
19. A. Sánchez de Miguel, C. C. M. Kyba, J. Zamorano, J. Gallego, K. J. Gaston, *Sci. Rep.* **10**, 7829 (2020).
20. S. D. Miller *et al*., *Remote Sens.* **5**, 6717–6766 (2013).
21. C. C. M. Kyba *et al*., *Sci. Adv.* **3**, e1701528 (2017).
22. A. Sánchez de Miguel, J. Bennie, E. Rosenfeld, S. Dzurjak, K. J. Gaston, *Remote Sens.* **13**, 3311 (2021).
23. A. Sánchez de Miguel *et al*., *Mon. Not. R. Astron. Soc.* **467**, 2966–2979 (2017).
24. C. C. M. Kyba, *Nat. Astron.* **2**, 267–269 (2018).
25. C. C. M. Kyba *et al*., *Sci. Rep.* **3**, 1835 (2013).
26. Materials and methods are available as supplementary materials.
27. A. Crumey, *Mon. Not. R. Astron. Soc.* **442**, 2600–2619 (2014).
28. N. Schulte-Römer, J. Meier, M. Söding, E. Dannemann, *Sustainability* **11**, 6160 (2019).
29. C. B. Luginbuhl, P. A. Boley, D. R. Davis, *J. Quant. Spectrosc. Radiat. Transf.* **139**, 21–26 (2014).
30. C. C. M. Kyba *et al*., *J. Geophys. Res. Atmos.* **127**, e2021JD036382 (2022).
31. J. C. Barentine *et al*., *J. Quant. Spectrosc. Radiat. Transf.* **253**, 107120 (2020).
32. C. C. M. Kyba, Y. O. Altıntaş, C. Walker, M. Newhouse, Software for analyzing Globe at Night data, GFZ Data Services (2022); https://doi.org/10.5880/GFZ.1.4.2022.008.
33. F. Falchi *et al*., Supplement to: The new world atlas of artificial night sky brightness. GFZ Data Services, (2016); https://doi.org/10.5880/GFZ.1.4.2016.001.

ACKNOWLEDGMENTS

We thank the thousands of participants in Globe at Night for their observations, which made this analysis possible. We thank K. Tockner for providing feedback on a draft and J. Hollan for producing the Globe at Night star charts. C.C.M.K. thanks A. Wisniewska for her 2012 visit to Berlin under the Erasmus student exchange program, which sparked his interest in Globe at Night and citizen science. We thank the referees for the suggestion to analyze DNB data at the observation locations. **Funding:** Globe at Night and C.E.W. are supported by an NSF Award (AST-1421197) to M. Mountain. C.C.M.K. acknowledges funding from the Federal Ministry of Education and Research, Germany (PT-Jülich under grant BMBF-033L038A), through the European Union's Horizon 2020 research and innovation program ERA-PLANET, grant agreement no. 689443 via the GEOEssential project, and from the Helmholtz Association Initiative and Networking Fund under grants ERC-RA-0031 and CS-0003. **Author contributions:** C.C.M.K. developed the analysis methodology and drafted the manuscript. C.C.M.K. and Y.O.A. wrote analysis software. Y.O.A. produced the figures. C.E.W. initiated and manages the Globe at Night project. M.N. manages the Globe at Night database. All authors contributed to writing and editing the manuscript. **Competing interests:** C.E.W. is a director of the International Dark-Sky Association, and C.C.M.K. is a former director of the same body. We declare that there are no other competing interests. **Data and materials availability:** The Globe at Night web application is at https://www.globeatnight.org/webapp/, and the data are available at https://www.globeatnight.org/maps.php. The subset of the dataset we used, and our analysis code, are archived at Deutsches GeoForschungsZentrum Potsdam (GFZ) Data Services (*32*). We also used the World Atlas data (*33*).

SUPPLEMENTARY MATERIALS

science.org/doi/10.1126/science.abq7781
Materials and Methods
Figs. S1 to S3
Tables S1 and S2
References (*34*–*37*)

Submitted 11 May 2022; accepted 17 November 2022
10.1126/science.abq7781